molbank

MDPI

Short Note

(1*RS*,2*RS*,6*RS*)-2-(6-Amino-9*H*-purin-9-yl)-8-azaspiro[5.6]dodec-10-en-1-ol Dihydrochloride

Ildar R. Iusupov, Konstantin A. Lyssenko, Andrea Altieri and Alexander V. Kurkin *

Chemistry Department, Lomonosov Moscow State University, Leninskie Gory 1/3, 119991 Moscow, Russia
* Correspondence: kurkin@direction.chem.msu.ru

Abstract: The title compound (1*RS*,2*RS*,6*RS*)-2-(6-Amino-9*H*-purin-9-yl)-8-azaspiro[5.6]dodec-10-en-1-ol dihydrochloride was synthesized for the first time in two steps, the first of which was a regioselectivity of epoxide ring-opening reaction under the action of adenine, yielding N-tert-butoxycarbonyl-((1*RS*,2*RS*,6*RS*)-2-(6-amino-9*H*-purin-9-yl)-8-azaspiro[5.6]dodec-10-en-1-ol. By treating the latter with a saturated methanolic solution of hydrogen chloride, it was possible to obtain ((1*RS*,2*RS*,6*RS*)-2-(6-Amino-9*H*-purin-9-yl)-8-azaspiro[5.6]dodec-10-en-1-ol dihydrochloride. The features of the molecular and crystal structure of ((1*RS*,2*RS*,6*RS*)-2-(6-Amino-9*H*-purin-9-yl)-8-azaspiro[5.6]dodec-10-en-1-ol dihydrochloride are discussed based on X-ray diffraction studies. The product overall yield was 40% out of two steps and after purification by column chromatography and recrystallization. The product was characterized by ^{1}H-NMR, ^{13}C-NMR, IR spectroscopy, HRMS and X-ray.

Keywords: nitrogen heterocycles; spiro compound; adenine; ring-opening reaction

Citation: Iusupov, I.R.; Lyssenko, K.A.; Altieri, A.; Kurkin, A.V. (1*RS*,2*RS*,6*RS*)-2-(6-Amino-9*H*-purin-9-yl)-8-azaspiro[5.6]dodec-10-en-1-ol Dihydrochloride. *Molbank* **2022**, *2022*, M1495. https://doi.org/10.3390/M1495

Academic Editor: R. Alan Aitken

Received: 18 October 2022
Accepted: 11 November 2022
Published: 15 November 2022

1. Introduction

The development of new synthetic methodologies for the generation of biologically active compounds is a crucial tool for medicinal and organic chemists [1]. This is a complex and multifaceted process that requires deep knowledge, initiative and creativity. Recently, the synthesis of saturated heterocyclic compounds has gained attention, since these structures are most often found in natural products and their synthetic methods are of high interest for producing new attractive chemical scaffolds for the development of new therapeutic molecules [2]. Spirocyclic compounds occupy an important place among saturated heterocyclic compounds [3–5]. In fact, spirocyclic compounds are notable for their unique three-dimensional structures, conformational rigidity, as well as their broad biological activity [6–9]. In particular, azaspirocyclic systems characterized by varied spiro-rings fused at the C3 position of the derivative of the piperidine core represent privileged scaffolds with prevalence in numerous natural products (polyzonimine, nitropolyzonamine, horsfiline, (+)-nitramine, (+)-isonitramine, (−)-isonitramine and (−)-sibirine et al.) [6,7,10] and pharmacologically relevant drugs (for example, vesamicol binds with high affinity to the allosteric binding site of the vesicular acetylcholine transporter (VAChT) [8,9,11,12]. Interestingly, some synthetic spiro compounds have found applications as chiral ligands and chiral catalysts, such as SPINOL and SPRIX [13,14]. Their conformational restriction, imparted by the spiro-carbon, provides an excellent strategy to not only imprint the desired conformation for ligand–protein binding, therefore increasing the specificity and potency, but also for enhancing the molecular complexity and potentially to reduce the P450 inhibition, rendering a better bioavailability and metabolic stability of the target compound [15,16]. An interesting expansion of the chemical space of these spiro systems can be achieved by conjugating them with different nucleobases. Nucleosides are fundamental building blocks of biological systems that show a wide range of biological activity. Thus, the chemistry behind them has been extensively explored and developed. Particularly, part of this nucleoside chemistry has been dedicated to modifications for avoiding their

metabolic degradation due to enzymatic attacks either on the heterocyclic base and/or on the sugar moiety. A key strategy to avoid such metabolic degradations exploits the replacement of oxygen in the sugar portion of the nucleoside with a methylene unit, resulting in carbocyclic nucleoside analogues which are highly resistant to phosphorylases. Therefore, we focused on developing new nucleoside-like compounds based on this approach.

Earlier, while studying the regioselectivity of the epoxide ring-opening reaction of the derivative of oxaspiro[bicyclo[4.1.0]heptane-2,3′-oxepine] under the action of adenine (100 °C, DMF), we obtained only one regiosisomer of adeninospirane [17]. Herein, by extending this methodology to include the fragment of the analogue of (−)-sibirine, we report the efficient synthesis and structural characterization of (1*RS*,2*RS*,6*RS*)-2-(6-Amino-9*H*-purin-9-yl)-8-azaspiro[5.6]dodec-10-en-1-ol dihydrochloride.

2. Results

Epoxide **1** was synthesized according to previously developed procedures [18,19]. Hydrochloride **3** was synthesized in two stages (Scheme 1). Epoxide **1** interacts with adenine when heated in a closed vessel, which leads to the formation of amino alcohol **2** in a 42% yield. When the unsymmetrical epoxides open, the S_N2 nucleophilic substitution mechanism takes place, which implies the formation of two possible isomeric alcohols during the reaction. In our case, during the opening of the neopentyl fragment containing epoxide **1**, only one from two regioisomers was formed. The resulting alcohol **2** was treated with a methanolic solution of hydrogen chloride at room temperature; as a result, we isolated the target product-((1*RS*,2*RS*,6*RS*)-2-(6-Amino-9*H*-purin-9-yl)-8-azaspiro[5.6]dodec-10-en-1-ol dihydrochloride (**3**). The synthesized hydrochloride **3** was isolated as a light brown powder.

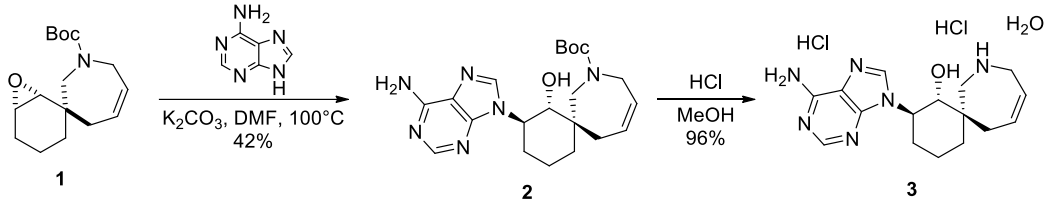

Scheme 1. The opening of epoxide **1** with adenine and synthesis of ((1*RS*,2*RS*,6*RS*)-2-(6-Amino-9*H*-purin-9-yl)-8-azaspiro[5.6]dodec-10-en-1-ol dihydrochloride (**3**).

The structure of the target product **3** was confirmed by ^{1}H, ^{13}C, HR-MS and IR spectroscopy (see Supplementary Materials). The ^{1}H, HR-MS, HMBC, HSQC, ROESY and COSY NMR and IR spectroscopy established the chemical formula of compound **2**. The ^{13}C-NMR spectrum of **2** showed signals of carbamate rotamers around the N-Boc group. The ^{1}H-NMR spectrum of **3** showed signals of an olefinic protons at 5.60–5.68 ppm and 5.87–5.96 ppm, signals of protons in the adenine (two C-H signals) fragment at 8.51 ppm and at 8.63 ppm, respectively. The characteristic signals of the C=C double bond in the ^{13}C-NMR spectrum were 123.2 ppm and 131.2 ppm, and the CH-OH carbon's signal in the carbocyclic fragment was 78.7 ppm.

The IR spectrum reveals that there were characteristic bands of the amino group of the purine fragment (3304 and 3144 cm^{-1}), OH group (1689 cm^{-1}) and C=N, C=C double bonds (1510–1605 cm^{-1}).

The molecular structure of compound **3** is illustrated in Figure 1 according to the X-ray diffraction data. The X-ray profiling showed that the compound crystallized as a dichloride salt and contained one molecule of water. A deep analysis of the long bonds and the Fourier synthesis difference showed that the protonation in the crystal is observed for both the nitrogen atom of the spirocycle and for the nitrogen atom $N_{(1)}$. In this particular case, a very unusual supramolecular organization was observed in the crystal: the formation of a tetracationic dimer.

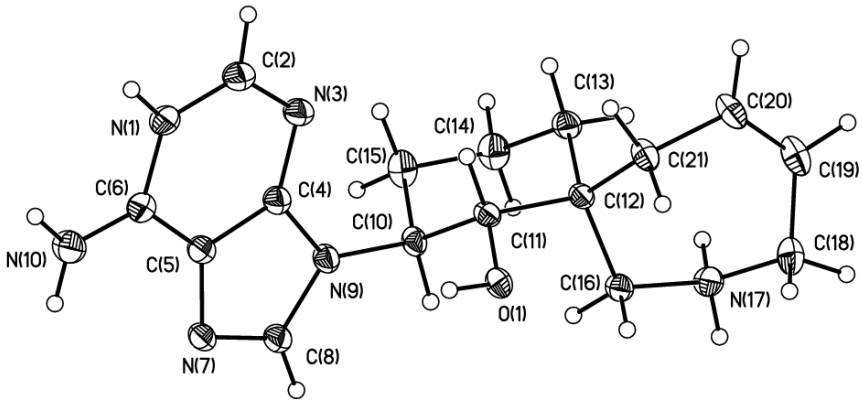

Figure 1. The molecular structure of dication **3**. Displacement ellipsoids are shown at a 50% probability level.

This centrosymmetric dimer, evidently unfavorable from an electrostatic point of view, is stabilized by two OH ... N(7) hydrogen bonds (2.908(2)Å) and two intermolecular H-bonds N(10)-H ... O(1) (N...O 2.872(2) Å) (Figure 2). Taking into account that the hydroxyl group acts in this supramolecular system as both a donor and an acceptor of a proton, it is logical to assume that, due to cooperative effects, the O–H ... N hydrogen bond will be additionally strengthened.

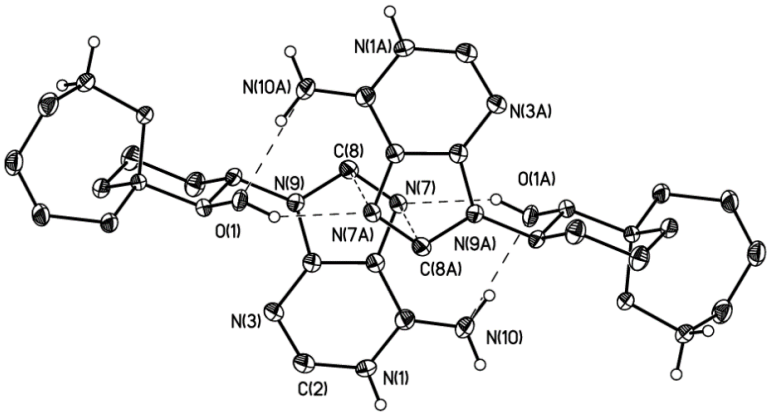

Figure 2. Centrosymmetric tetracationic dimer in crystal **3** (hydrogen atoms of C-H groups are not shown).

In addition to the H-bonds, this dimer is also stabilized due to stacking interactions. Although the overlapping area of the purine rings is not large, the distance between the parallel planes of the purine rings is only 3Å, and the shortest N(7) ... C(8) contacts are 3.077(2) Å. Evidently, for a given tetracationic dimer, it is impossible to estimate the stabilization energy by standard methods of quantum chemistry, since for charged supramolecular associates formed by fragments with the same charges, the dimer is inevitably unstable in the gas phase. Therefore, to assess its stabilization, we used an approach based on the use of a topological analysis of the electron density distribution function, in combination with the Espinosa–Lecomte empirical correlation [20,21]. The electron density distribution function (ρ(r)) was obtained for the experimental geometry, for which the optimization of the positions of the hydrogen atoms was carried out in the framework of the PBE1PBE/def-2-TZVP calculation. According to the topological analysis of ρ(r) in the framework of the "Atoms in the Molecule" theory, the critical points (3,−1) were localized both for all hydrogen bonds and for the stacking interaction. All of these nonvalent interactions in the dimer correspond to interactions of the closed shell type. The energy of the O-H ... N bonds is 6.6 kcal/mol, and for N-H ... O it is 9.8 kcal/mol. The stacking interaction is expectedly weaker and its total energy is 3.8 kcal/mol. Thus, the total stabilization of the dicationic

dimer will be 36 kcal/mol. It seems that such a high stabilization energy is sufficient to stabilize the dimer despite the significant positive charge of the supramolecular associate.

3. Materials and Methods

3.1. General

Reagents were purchased at the highest commercial quality and used without further purification unless otherwise stated. Reactions were monitored by thin-layer chromatography (TLC) carried out on Merck TLC (Moscow, Russia) Silica gel plates ($60F_{254}$), using UV light for visualization and basic aqueous potassium permanganate or iodine fumes as developing agents. ^{1}H and ^{13}C NMR spectra were recorded on Bruker Avance 400 instrument (Moscow, Russia) with an operating frequency of 400 and 100 MHz, respectively, and calibrated using residual undeuterated chloroform (δH = 7.26 ppm) and $CDCl_3$ (δC = 77.16 ppm), or undeuterated DMSO (δH = 2.50 ppm) and DMSO-d_6 (δC = 39.51 ppm) as internal references. The following abbreviations are used to set multiplicities: s = singlet, d = doublet, t = triplet, q = quartet, quint = quintet, m = multiplet, br. = broad. For structure determination and NMR signal assignment in **2** 2D correlation spectra, ^{1}H-^{1}H (COSY, ROESY) and ^{1}H-^{13}C (HSQC, HMBC) were used. IR spectra were recorded on Thermo Nicolet IR-200 in KBr, nujol or neat. High-resolution mass spectra (HRMS) were recorded on a TripleTOF 5600 mass spectrometer (AB Sciex, Concord, ON, Canada) equipped with a DuoSpray ion source. Low-resolution mass spectra were recorded on Finnigan MAT mass spectrometer using electron ionization (direct inlet) and an ITD-700 detector with the ionizing electron energy being 70 eV and the mass range being m/z 35–400. Elemental analysis was performed on EURO EA CHN Elemental Analyzer. The melting points (m.p.) were measured in open capillaries and presented without correction.

3.2. Synthesis of Tert-butyl (1RS,2RS,6RS)-2-(6-Amino-9H-purin-9-yl)-1-hydroxy-8-azaspiro[5.6]dodec-10-ene-8-carboxylate (2)

Epoxide **1** (0.50 g, 1.79 mmol, 1 eq) was dissolved in abs. DMF (18 mL, 0.1 M) and K_2CO_3 (0.741 g, 5.37 mmol, 3 eq) and adenine (0.484 g, 3.58 mmol, 2 eq) were added. The reaction mixture was heated at 110–120 °C for 30 h until complete disappearance of the starting epoxide by TLC (usually 25–30 h). The reaction mixture was cooled to room temperature, poured into water (50 mL) and extracted with EtOAc (3 × 50 mL). The combined organic layers were dried over Na_2SO_4, filtered and evaporated. The resulting substance was purified by flash chromatography (gradient elution with CH_2Cl_2-MeOH systems from 20:1 to 10:1). Yield 0.31 g (42%), beige crystals (yellow oil, crystallizing on storage), m.p. 220–225 °C (octane). R_f = 0.4 in CH_2Cl_2-MeOH (10:1). ^{1}H-NMR (DMSO-d_6, δ_H): 1.03–1.15 (m, 1H), 1.41 (d, J = 13.4 Hz, 9H), 1.47–1.62 (m, 1H), 1.68–2.02 (m, 4H), 2.06–2.25 (m, 1H), 2.34–2.69 (m, 1H), 3.38–4.42 (m, 6H), 4.89 (dd, J = 23.0, 7.6 Hz, 1H), 5.58–5.78 (m, 2H), 7.11 (d, J = 2.3 Hz, 2H), 8.10 (s, 1H), 8.13 (d, J = 6.7 Hz, 1H). ^{13}C-NMR (mixture of rotamers), δ_C: (20.1, 20.5), (28.1, 28.2, 3 C), (31.0, 31.3), (32.1, 32.9), (37.6, 38.8), (44.3, 44.7), (46.7, 46.9), (47.5, 47.9), (56.6, 56.8), (77.1, 77.7), (79.2, 79.2), 119.2, (126.9, 127.6), (129.3, 129.6), 140.7, 149.8, 152.0, (155.1, 155.4), 156.0. IR ν_{max} (CM^{-1}): 3123, 2931, 2882, 2851, 1695, 1666, 1596, 1572, 1480, 1453, 1412, 1366, 1303, 1248, 1207, 1170, 1142, 1114, 1071, 892, 883, 798, 789, 767, 756, 653, 623, 602. HR-MS (ESI-TOF): 415.2458 ([M + H]$^+$, $C_{21}H_{31}N_6O_3$; calcd 415.2452). Copies of ^{1}H-NMR, ^{13}C-NMR, 2D correlation spectra ^{1}H-^{1}H (COSY, ROESY) and ^{1}H-^{13}C (HSQC, HMBC) and mass spectra of **2** are presented in Supplementary Materials.

3.3. Synthesis of Dihydrochloride of (1RS,2RS,6RS)-2-(6-Amino-9H-purin-9-yl)-8-azaspiro[5.6]dodec-10-en-1-ol (3)

To alcohol **2** (0.20 g, 0.482 mmol, 1.0 eq) in MeOH (5 mL) was added a methanolic solution of hydrogen chloride (20 mL, 1M HCl, the solution was preliminarily prepared by adding acetyl chloride to methanol dropwise with cooling). The reaction mixture was allowed to stir at room temperature for 30 min and then rotary evaporated. Et_2O (40 mL) was added, the precipitate was filtered off and air dried. Yield 0.18 g (96%), light brown

crystals, m.p. 300–305 °C (methanol). ^{1}H-NMR (DMSO-d_6, δ_H): 1.16–1.31 (m, 1H), 1.43–1.67 (m, 2 H), 1.86–2.20 (m, 4 H), 2.93 (d, J = 13.3 Hz, 1H), 3.26–3.41 (m, 2H), 3.54–3.73 (m, 2H), 3.86 (d, J = 10.5 Hz, 1H), 4.45–4.55 (m, 1H), 5.60–5.68 (m, 1H), 5.87–5.96 (m, 1H), 8.51 (s, 1H), 8.63 (s, 1H), 8.72–9.55 (M, 4 H). ^{13}C-NMR, δ_C: 19.6, 30.6, 32.0, 36.6, 42.5, 46.0, 47.9, 57.2, 76.7, 118.0, 123.2, 131.2, 143.4, 144.5, 148.7, 150.5. IR ν_{max} (CM^{-1}): 3304, 3144, 3052, 2943, 2788, 2659, 1689, 1605, 1584, 1510, 1469, 1459, 1417, 1382, 1306, 1206, 1060, 886, 784, 695, 678, 637, 619. HR-MS (ESI-TOF): 315.1932 ([M-2HCl + H]$^+$, $C_{16}H_{23}N_6O$; calcd 315.1928).

3.4. Crystallography Details

X-ray crystallography study of the crystals were carried out on a Bruker Quest D8 diffractometer equipped with a Photon-III detector using ϕ,ϖ-scans of narrow (0.5°) frames with Mo K_α radiation (λ = 0.71073 Å) and a graphite monochromator. The structure was solved by direct methods using the SHELXT-2014/5 [22] and was refined by the full-matrix least-squares method against all F^2 in anisotropic approximation using the SHELXL-2018/3 [23]. The hydrogen atom positions were calculated with the riding model. Absorption corrections were applied using the empirical multi-scan method with the SADABS program [24]. The hydrogen atoms of the NH and OH groups are localized from Fourier electron density syntheses. All other hydrogen atoms were placed in the calculated positions and refined according to the rider model. An analysis of the difference syntheses of electron density and atomic displacement parameters showed that the solvate water molecule is disordered over two positions with occupancies 0.548(7) and 0.452(7). The compound was triclinic, space group P-1, a = 7.3638(4), b = 10.7327(6), c = 13.0314(8)Å, α = 110.036(2)°, β = 105.026(2)°, γ = 92.097(2)°, V = 925.53(9) Å^3, Z = 2, $C_{16}H_{26}Cl_2N_6O_2$, Dc = 2.230 r/cm^3, μ = 1.454 mm^{-1}, F(000) = 428, independent reflections 5382, wR2 = 0.1513, S = 1.04 for all reflections (R = 0.0589 for 3921 I > 2σ). Tables listing detailed crystallographic data, atomic positional parameters and bond lengths and angles are available as CCDC 2122336 from the Cambridge Crystallographic Data Centre via www.ccdc.cam.ac.uk/data_request/cif (accessed on 16 November 2021).

4. Conclusions

The interaction of adenine with spirocycle **1** in DMF led to the epoxide ring-opening product **2** upon treatment of it with a saturated methanolic solution of hydrogen chloride. We successfully obtained the target compound ((1*RS*,2*RS*,6*RS*)-2-(6-Amino-9*H*-purin-9-yl)-8-azaspiro[5.6]dodec-10-en-1-ol dihydrochloride in gram quantitates, good purity and with a 40% preparative yield in two steps.

Supplementary Materials: The following data are available online. ^{1}H-NMR, ^{13}C-NMR, 2D correlation spectra ^{1}H-^{1}H (COSY, ROESY), ^{1}H-^{13}C (HSQC, HMBC) and HR-MS of **2** and **3**.

Author Contributions: I.R.I. performed the chemical synthesis. The registration and interpretation of the NMR data and structure characterization of both compounds were conducted by I.R.I. and A.A. X-ray crystallography study of the crystals was carried out by K.A.L. The manuscript was written by A.V.K., A.A. and K.A.L. All authors have read and agreed to the published version of the manuscript.

Funding: The current work was financially supported by the Russian Foundation for Basic Research (Grant No. 20-33-90036).

Institutional Review Board Statement: Not applicable.

Informed Consent Statement: Not applicable.

Data Availability Statement: Not applicable.

Acknowledgments: The study was performed using equipment purchased at the expense of the Development Program of Moscow State University. High-resolution mass spectra were recorded at the Department of Structural Studies, N.D. Zelinsky Institute of Organic Chemistry of the Russian Academy of Sciences, Moscow.

Conflicts of Interest: The authors declare no conflict of interest.

References

1. Campbell, I.B.; Macdonald, S.J.F.; Procopiou, P.A. Medicinal chemistry in drug discovery in big pharma: Past, present and future. *Drug Discov.* **2018**, *23*, 219–234. [CrossRef] [PubMed]
2. Vo, C.-V.T.; Bode, J.W. Synthesis of Saturated N-Heterocycles. *J. Org. Chem.* **2014**, *79*, 2809–2815. [CrossRef] [PubMed]
3. Zheng, Y.-J.; Tice, C.M. The utilization of spirocyclic scaffolds in novel drug discovery. *Expert Opin. Drug Discov.* **2016**, *11*, 831–834. [CrossRef]
4. Zheng, Y.; Tice, C.M.; Singh, S.B. The use of spirocyclic scaffolds in drug discovery. *Bioorg. Med. Chem. Lett.* **2014**, *24*, 3673–3682. [CrossRef] [PubMed]
5. Galliford, C.V.; Scheidt, K.A. Pyrrolidinyl-spirooxindole natural products as inspirations for the development of potential therapeutic agents. *Angew. Chem. Int. Ed.* **2007**, *46*, 8748–8758. [CrossRef]
6. Wanner, J.W.; Koomen, G.J. *Studies in Natural Products Chemistry: Stereoselectivity in Synthesis and Biosynthesis of Lupine and Nitraria Alkaloids*; Atta-ur-Rahman, Ed.; Elsevier: Amsterdam, The Netherlands, 1994; p. 731.
7. Boubaker, J.; Bhouri, W.; Sghaier, B.M.; Bouhlel, I.; Skandrani, I.; Ghedira, K.; Chekir-Ghedira, L. Leaf extracts from Nitraria retusa promote cell population growth of human cancer cells by inducing apoptosis. *Cancer Cell Int.* **2011**, *11*, 37. [CrossRef]
8. Ye, N.; Chen, H.; Wold, E.A.; Shi, P.-Y.; Zhou, J. Therapeutic Potential of Spirooxindoles as Antiviral Agents. *ACS Infect Dis.* **2016**, *10*, 382–392. [CrossRef]
9. Liebowitz, S.M.; Belair, E.J.; Witiak, D.T.; Lednicer, D. Synthesis and cardiovascular activity of a series of spiroureas. *Eur. J. Med. Chem.* **1986**, *21*, 439–444.
10. Yang, J.; Park, Y.; Yang, S.; Lee, G.; Ha, M.W.; Kim, M.-H.; Hong, S.; Park, H.-G. Enantioselective Total Synthesis of Nitraria Alkaloids: (+)-Nitramine, (+)-Isonitramine, (−)-Isonitramine, and (−)-Sibirine via Asymmetric Phase-Transfer Catalytic α-Allylations of α-Carboxylactams. *J. Org. Chem.* **2021**, *86*, 4375–4390. [CrossRef]
11. Altar, C.A.; Marien, M.R. [3H]vesamicol binding in brain: Autoradiographic distribution, pharmacology, and effects of cholinergic lesions. *Synapse* **1988**, *2*, 486–493. [CrossRef]
12. Marshall, G.; Parsons, S.M. The vesicular acetylcholine transport system. *Trends Neurosci.* **1987**, *10*, 174–177. [CrossRef]
13. Bajracharya, G.B.; Arai, M.A.; Koranne, P.S.; Suzuki, T.; Takizawa, S.; Sasa, H. Development of Chiral Spiro Ligands for Metal-Catalyzed Asymmetric Reactions. *Bull. Chem. Soc. Jpn.* **2009**, *82*, 285–302. [CrossRef]
14. Bajracharya, G.B. Design and Synthesis of Chiral Spiro Ligands. *J. Nepal Chem. Soc.* **2013**, *28*, 1–23. [CrossRef]
15. Veber, D.F.; Johnson, S.R.; Cheng, H.Y.; Smith, B.R.; Ward, K.W.; Kopple, K.D. Molecular properties that influence the oral bioavailability of drug candidates. *J. Med. Chem.* **2002**, *45*, 2615–2623. [CrossRef] [PubMed]
16. Lovering, F. Escape from flatland 2: Complexity and promiscuity. *ChemMedComm* **2013**, *4*, 515–519. [CrossRef]
17. Iusupov, I.R.; Lukyanenko, E.R.; Altieri, A.; Kurkin, A.V. Design and Synthesis of Fsp3-enriched Spirocyclic-Based Biological Screening Compound Arrays via DOS strategies and their NNMT Inhibition Profiling. *ChemMedChem.* **2022**. [CrossRef]
18. Castro, S.; Camarasa, M.-J. Polypharmacology in HIV inhibition: Can a drug with simultaneous action against two relevant targets be an alternative to combination therapy? *Eur. J. Med. Chem.* **2018**, *150*, 206–227. [CrossRef]
19. Belov, D.S.; Lukyanenko, E.R.; Kurkin, A.V.; Yurovskaya, M.A. Highly Stereoselective and Scalable Synthesis of trans-Fused Octahydrocyclohepta[b]pyrrol-4(1H)-ones via the Aza-Cope–Mannich Rearrangement in Racemic and Enantiopure Forms. *J. Org. Chem.* **2012**, *77*, 10125–10134. [CrossRef]
20. Espinosa, E.; Alkorta, I.; Elguero, J.; Molins, E. From weak to strong interactions: A comprehensive analysis of the topological and energetic properties of the electron density distribution involving X–H···F–Y systems. *J. Chem. Phys.* **2002**, *117*, 5529–5542. [CrossRef]
21. Espinosa, E.; Molins, E.; Lecomte, C. Hydrogen bond strengths revealed by topological analyses of experimentally observed electron densities. *Chem. Phys. Lett.* **1998**, *285*, 170–173. [CrossRef]
22. Sheldrick, G.M. SHELXT—Integrated space-group and crystal-structure determination. *Acta Cryst.* **2015**, *A71*, 3–8. [CrossRef] [PubMed]
23. Sheldrick, G.M. Crystal structure refinement with SHELXL. *Acta Cryst.* **2015**, *C71*, 3–8.
24. *SADABS*, version 2008-1; Bruker AXS: Madison, WI, USA, 2008.